Upgrades to the Fluorescence Detectors of the Pierre Auger Observatory

THE UNIVERSITY *of* ADELAIDE

Tristan William Sudholz

School of Physical Sciences
University of Adelaide

This dissertation is submitted for the degree of
Doctor of Philosophy

April, 2019

Declaration

I, Tristan William Sudholz, certify that this work contains no material which has been accepted for the award of any other degree or diploma in any university or other tertiary institution and, to the best of my knowledge and belief, contains no material previously published or written by another person, except where due reference has been made in the text. In addition, I certify that no part of this work will, in the future, be used in a submission for any other degree or diploma in any university or other tertiary institution without the prior approval of the University of Adelaide and where applicable, any partner institution responsible for the joint-award of this degree.

I give consent to this copy of my thesis, when deposited in the University Library, being made available for loan and photocopying, subject to the provisions of the Copyright Act 1968.

I also give permission for the digital version of my thesis to be made available on the web, via the Universitys digital research repository, the Library catalogue and also through web search engines, unless permission has been granted by the University to restrict access for a period of time.

Tristan William Sudholz

Abstract

Acknowledgements

Contents

Nomenclature

PAO	Pierre Auger Observatory
EAS	Extensive Air Shower
NSB	Night Sky Background
PE	Photo-electron
FD	Fluorescence Detector
SD	Surface Detector
PMT	Photomultiplier Tube
FLT	First Level Trigger

Introduction

- Define Cosmics Rays.
- The origins of the highest energy cosmic-rays still unknown.
- First detection by Pierre Auger in 1937 and the current detector looking at theses energies is the Pierre Auger Observatory.
- Hybrid experiment containing both surface detectors and fluorescence detectors
- Surface detector has nearly 100% up-time while the fluorescence detectors only have 15% up-time.
- **** Proposal to extend the fluorescence detector up-time. To achieve this will have to operator while the moon is above the horizon. This will increase the level NSB and will have the PMTs run under a reduced gain to compensate. ****
- Photomultiplier Tubes are used as pixels within the camera of the fluorescence detectors and the aim of these thesis is to quantify the characteristics of the PMT under the reduced gain and increased.
- Outline a Summary of each chapter.

Cosmic-rays are particles that originate outside of the Earth atmosphere. These particles can be photons, hadronic or leptonic in nature [ref?]. In this thesis, when mentioning cosmic-rays I will mean the hadronic component unless specified otherwise. Cosmic-rays have been measurement over a large range of energies (over 6 decades in energy) and it has many interesting features have been observed in this energy spectrum. One of the longest running mysteries is what happens at the highest energy. Since the first detection of extensive air showers by Pierre Auger in 1937 [ref], many different experiments have endeavoured to solve this mystery. The Pierre Auger Observatory [ref] is currently in operation to observe cosmic-rays at the highest energies.

The Pierre Auger Observatory is a hybrid experiment consisting of both surface detectors and fluorescence detectors. (Outline location) The surface detector has a nearly 100% operation up-time ref while the fluorescence detectors only 15% operation up-time [ref]. (Outline how PAO detects cosmic-rays, just need a brief summary).

A current proposal to extend the fluorescence detector operation up-time. Extended up-time would be beneficial as the fluorescence detectors image the entire extensive air shower and would increase the number of showers observed through out yearly observation. To achieve the extended operation the fluorescence detectors would have to operated while the moon is above the horizon. While the moon is up, this would increased the Night Sky Background level and to compensate the Photomultiplier Tubes acting as the camera pixels would have to be run under reduced gain.

The aim of this thesis is to quantify the characteristics of the Photomultiplier Tubes operating under this reduced gain and outline any operation strategies. Outline of each chapter is as follows:

- Chapter 1: Cosmic-rays

  Does this work as a new line

- Chapter 2: Detection of Cosmic-Rays

  Add text here

- Chapter 3: The Pierre Auger Observatory

  Add text here

- Chapter 4 : EAS Selection Efficiency with Increased NSB

  Add text here

- Chapter 5 : Quantifying Characteristics of the FD PMT

  Add text here

- Chapter 6 : Computer Simulation of the FD PMT

  Add text here

- Chapter 7 : Measuring Gain Variance of the FD PMT with CalA data

  Add text here

- Chapter 8 : Laboratory Simulation of FD Shifts

  Add text here

- Chapter 9 : Effectiveness of Cloud Camera Cuts

  Add text here

- Chapter 10: Conclusion

  Future Work

Chapter 1

Cosmic-Rays

1.1 History of Cosmic-Rays

First detection of ionizing radiation.

1785: Coulomb found that electroscopes can spontaneously discharge by the action of the air and not by defective insulation

1835: Faraday confirms the observation by Coulomb, with better insulation technology

1879: Crookes measures that the speed of discharge of an electroscope decreased when pressure was reduced

1.2 Energy Spectrum and Mass composition

Cosmic-rays have been detected over a large range of energies from GeV (10^9 eV) to above EeV (10^18 eV). Spectrum in Figure 1.1 shows the break at the knee and ankle and which type of experiments are most suited to measurement each part. Cosmic-ray spectrum starts out at E^{-2} and can be as steep as $E^{-2.7}$ at the highest energies.

Cosmic-rays can consist of protons to iron.

1.3 Production Method and Sources

Supernova explosions

AGN jets

other energetic processes

dark matter annihilations.

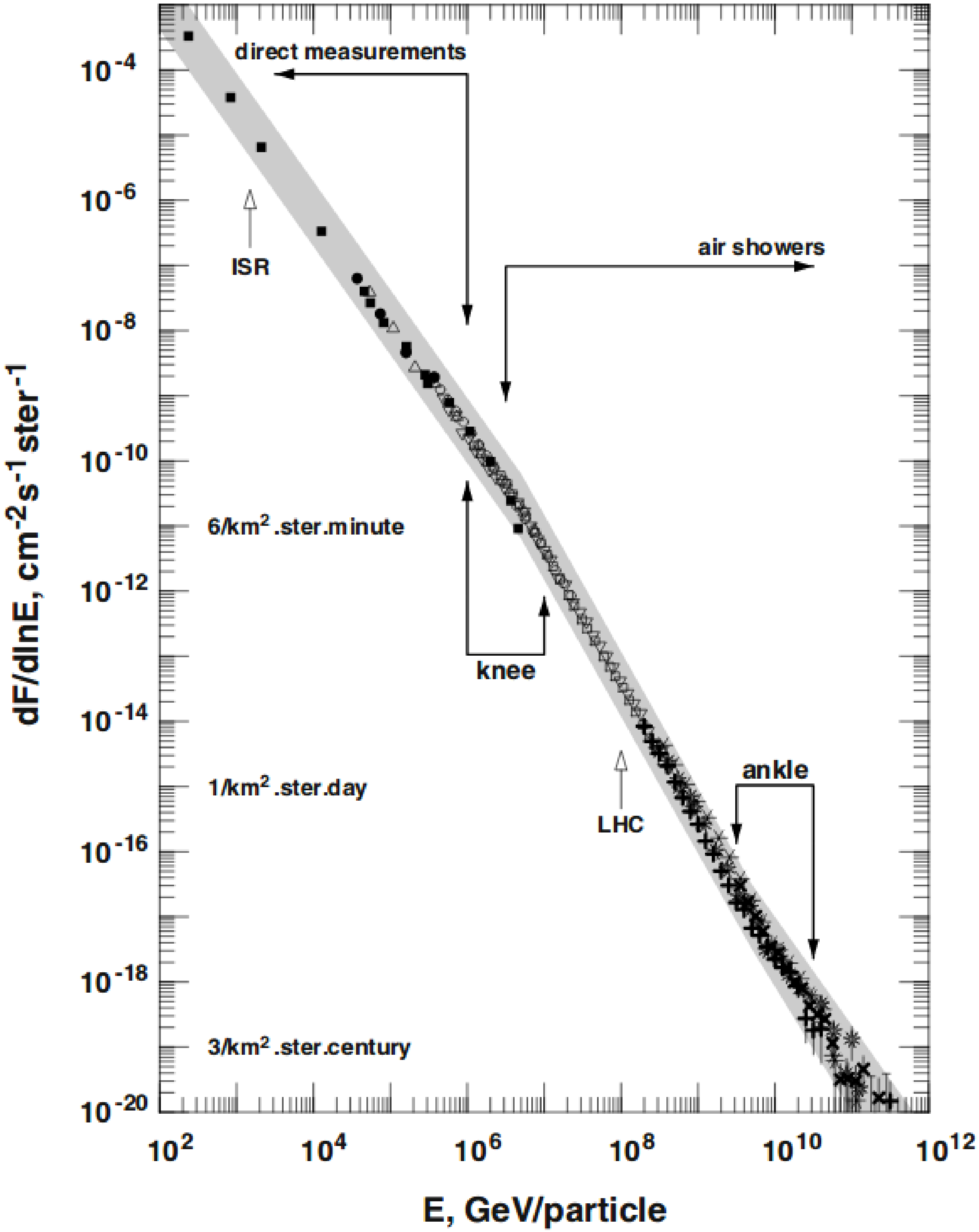

Figure 1.1: Measured energy spectrum of cosmic-rays from 100 GeV up to the highest detected energy.

Chapter 2

Detections of Cosmic-Rays

2.1 Extensive Air Showers

Use Earth's atmosphere as an interaction medium. Primary particle interacts with the molecules in the atmosphere to produce a cascade of secondary particles. This cascade of particles is referred to as an Extensive Air Shower (EAS). Hadronic primaries can produce pions, muons and other stuff. Mixture of a hadronic core with an electromagnetic component from the decay of π^0.

Shower profile has particles produced until energy on individual secondary particles drop below the ionization threshold. Therefore the shower will reach a point of maximum particle number then will drop off.

2.2 Fluorescence Production

The charge particles of EAS interact with the nitrogen molecules in the atmosphere. This interaction turns the nitrogen molecule dipole like and when the nitrogen returns to a ground state, a photon is emitted. This emitted photon is termed fluorescence light. Fluorescence light is can be emitted isotropically and typically in the UV band (between 300 and 400 nm). *** Show wavelength profile ***

2.3 Atmospheric Effects

2.4 Detectors and History

Early Experiments:

Volcano Ranch

Haverah Park

SUGAR

Yakutsk array is located in Russia and has been operating in different forms since 1967. The array reached a maximum collecting area of 17 km^2 around 1990. Recently it has been reconfigured to have a collection area of 8 km^2 to study lower energy cosmic-rays.

Akeno Gaint Air Shower Array (AGASA) is located in Tokyo, Japan. Operating at an average altitude of 667 m above sea level from 1990 to 2004. The array consist of over one hundred scintillator detectors covering 100 km^2 ***check this***. The timing measurements and data collection is achieved via interconnected optical fibers.

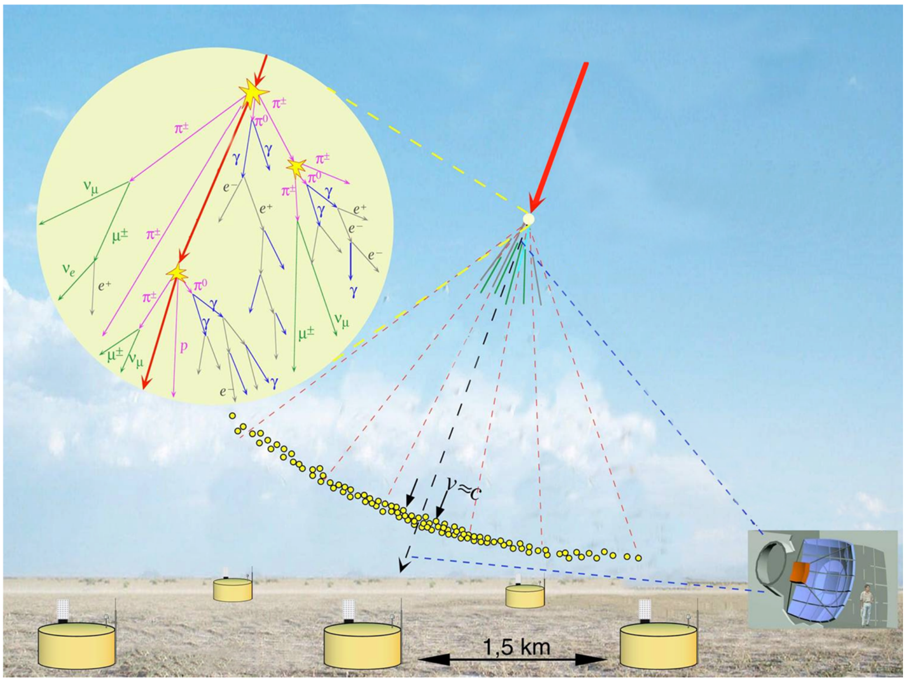

Figure 2.1: Diagram of Cosmic-ray Extensive Air Showers.

The Fly's Eye was the first successful air fluorescence detector operating from 1981 to 1993 at the Dugway Proving Grounds in Utah, USA. Fly's Eye achieved a time averaged aperture of about 100 km^{2}sr at the highest energies, considering it only operated on clear moonless nights.

HiRes improved on the Fly's Eye design by advancing resolution and sensitivity, This was achieved by increasing the telescope effective mirror area to 3.8 m^2 and reducing the camera pixel angular diameter to 1°.

Chapter 3

Pierre Auger Observatory

Science Goals of the Pierre Auger Observatory is to probe the origins and characteristics of cosmic rays above 10^{17} eV and to study the interactions of the most energetic particles observed in nature.

The Pierre Auger Observatory (PAO) is an hybrid detector that is located near Malargüe in the Mendoza Province, Argentina. PAO consists of 1660 Cherenkov water detector spread over 3000 km^2 by 24 fluorescence telescopes.

3.1 Surface Detector

The surface array consists of 1660 water Cherenkov tanks. The majority of tanks are configured with a spacing of 1500 metres while there is a small subset of tanks in front of the fluorescence telescopes at the Coihueco site with spacing of 750 metres.

The surface array has a duty cycle of nearly 100% and the maintenance cycle is so that no more then 20 tanks are down at any one time.

3.1.1 AugerPrime

3.2 Fluorescence Detector

There are four fluorescence detector site surrounding the surface array. At each fluorescence detector site there are six telescopes covering 180° in azimuth and 30° in elevation. At one site there are three extra telescopes with slightly greater then 90° in azimuth and cover 30° to 60° in elevation.

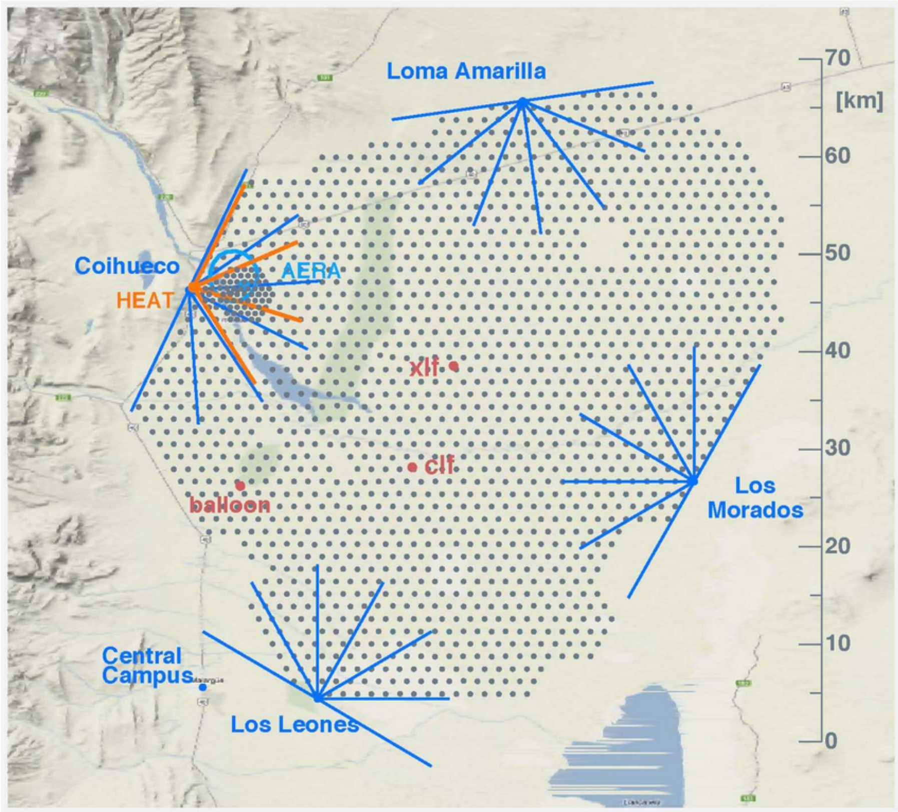

Figure 3.1: Image of layout of Pierre Auger Observatory located near Malargue, Argentina.

Figure 3.2: Image of one of the fluorescence detector site (background) and one of the surface detectors (foreground).

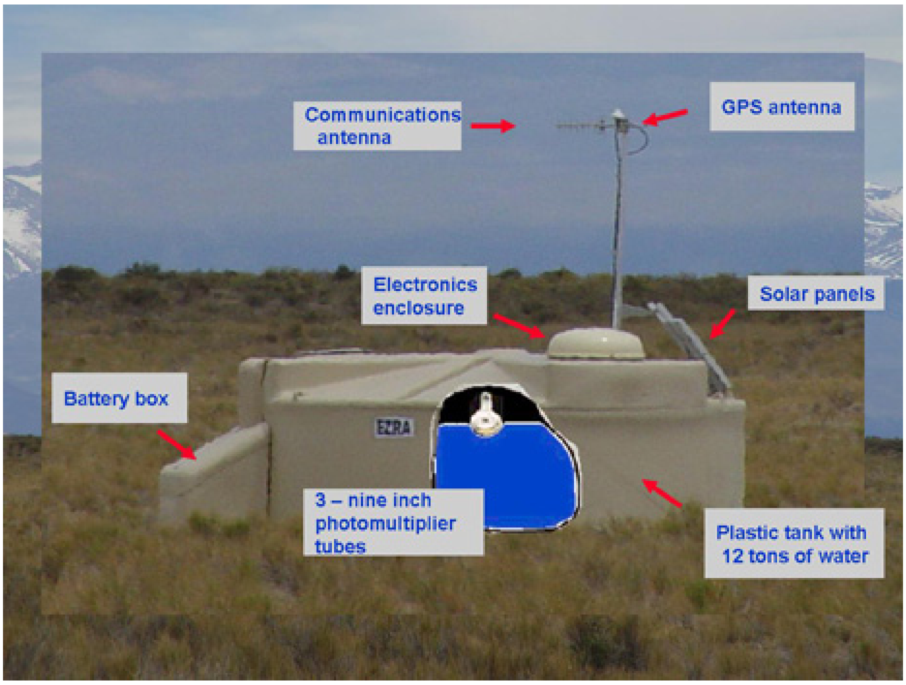

Figure 3.3: Basic schematic of a surface detector.

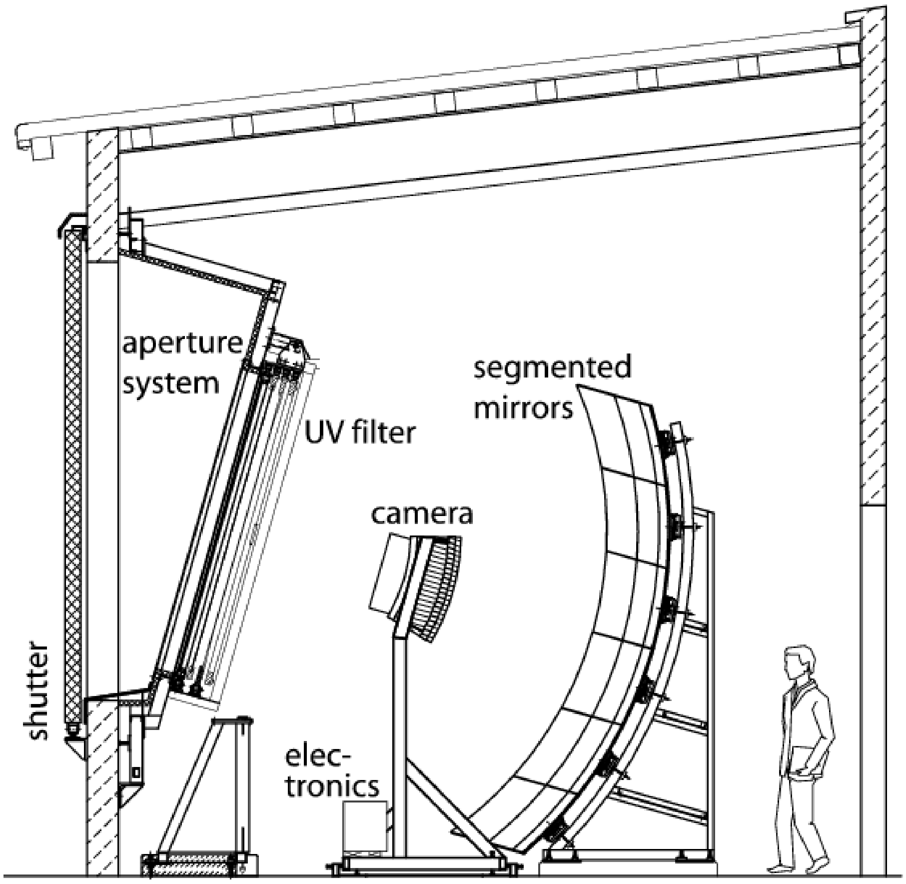

Figure 3.4: Basic schematic of a fluorescence telescope.

3.2.1 Photomultiplier Tubes

3.3 Communication System and CDAS

3.4 Event Reconstruction

3.4.1 Surface Detector

3.4.2 Fluorescence Detector

3.5 Enhancements and future upgrades

Chapter 4

EAS Selection Efficiency with Increased NSB

Selection Efficiency of EAS under increased NSB

- Smearing real data with extra noise
- Simulating EAS with an increased NSB
- Talk about differences in smearing and simulating EAS (different triggering conditions)
- Energy and Xmas resolution and bias
- Rp bias
- differences in track length

Typically the NSB measured at PAO is in Units of ADC^2. As the signal is AC coupled, this is the variance around the zero and is directly proportional to the fluctuations in the NSB. The average value of the NSB is:

$$\sigma^2 \sim 25\ \mathrm{ADC}^2 \tag{4.1}$$

Converting the variance into photons by using:

$$\sigma_{pe}^2 = [\sigma_{\mathrm{ADC}}^2]^{\mathrm{sky}}\ /\ \mathrm{A}_{\mathrm{G}}^2 \tag{4.2}$$

$$\mathrm{n}_{\mathrm{ph}} = \frac{\sigma_{pe}^2}{(1+\mathrm{V}_{\mathrm{G}})} \tag{4.3}$$

where σ_{pe} is the standard deviation of the photo-electron count, n_{ph} is the photon count and A_{G} is equal to:

$$\mathrm{A}_{\mathrm{G}} = \frac{1}{\mathrm{C}_{\mathrm{FD}}.\mathrm{f}.\mathrm{Q}} \tag{4.4}$$

where

A_{G} is the absolute gain (ADC/photo-electron)

C_{FD} is the FD pixel calibration constant.

Q is the Quantum efficiency of the PMT.

f is the efficiency if the telescope optics.

/*—— Find reference to number below ——*/
Assuming typical measured values for C_{FD}, Q and f shown in:

C_{FD}	4.5 photons/ADC
Q	0.29
f	0.465

Therefore can now calculate A_G from Eq. 4.4 and using

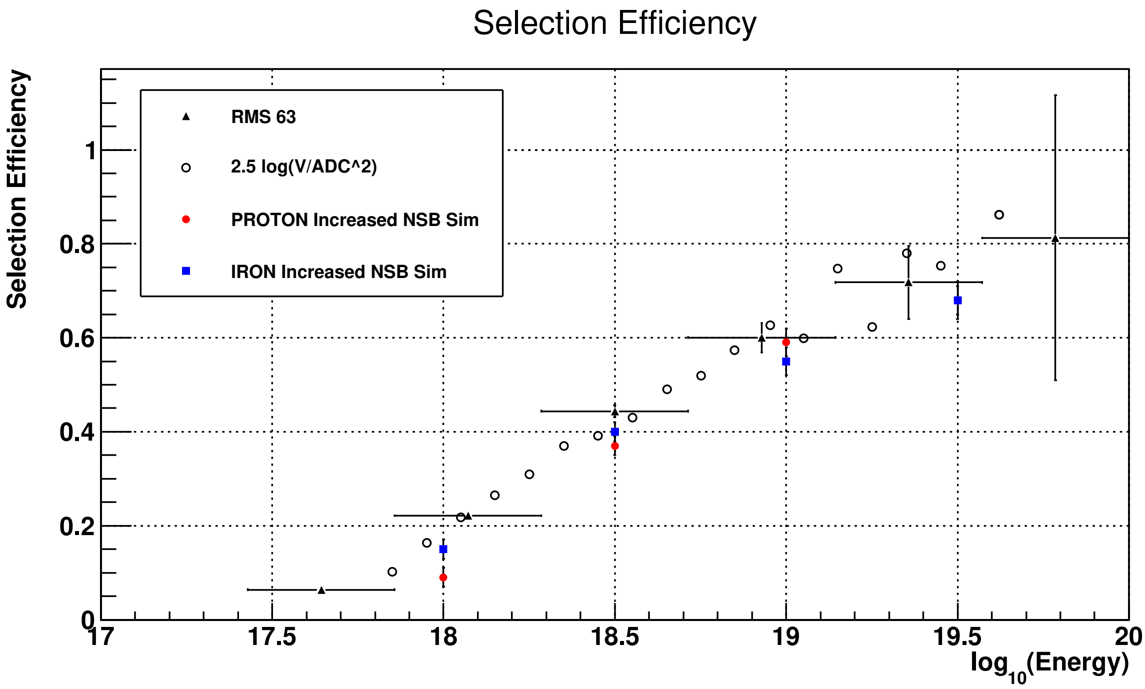

Figure 4.1: Selection Efficiency plot containing data from both the Smearing method and simulated showers. These results are compared to the work done by M. Unger.

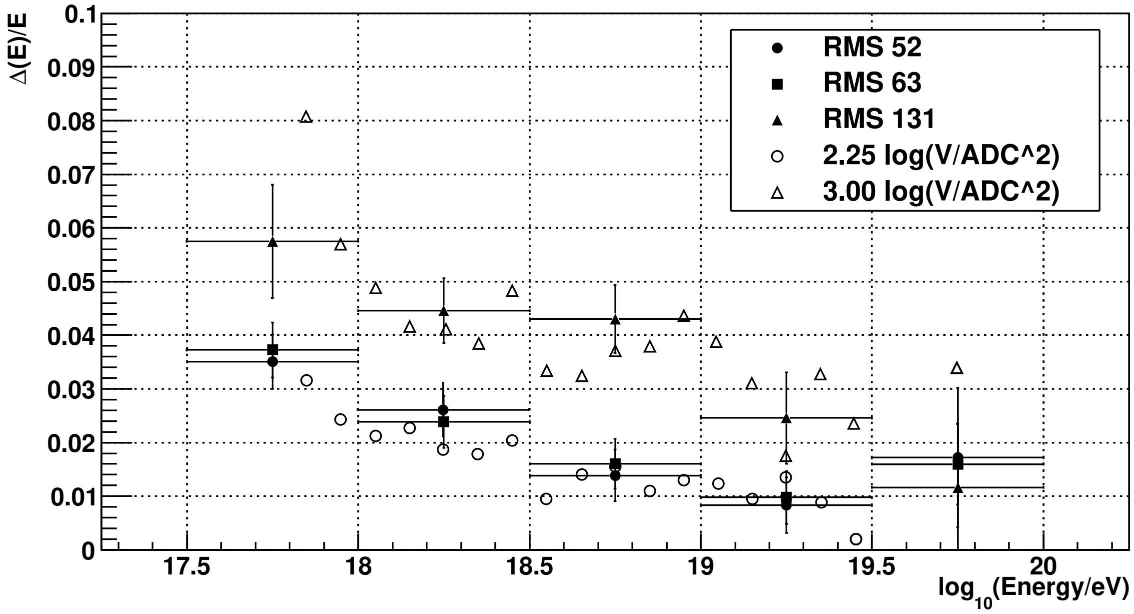

Figure 4.2: Energy Bias using Smearing Method.

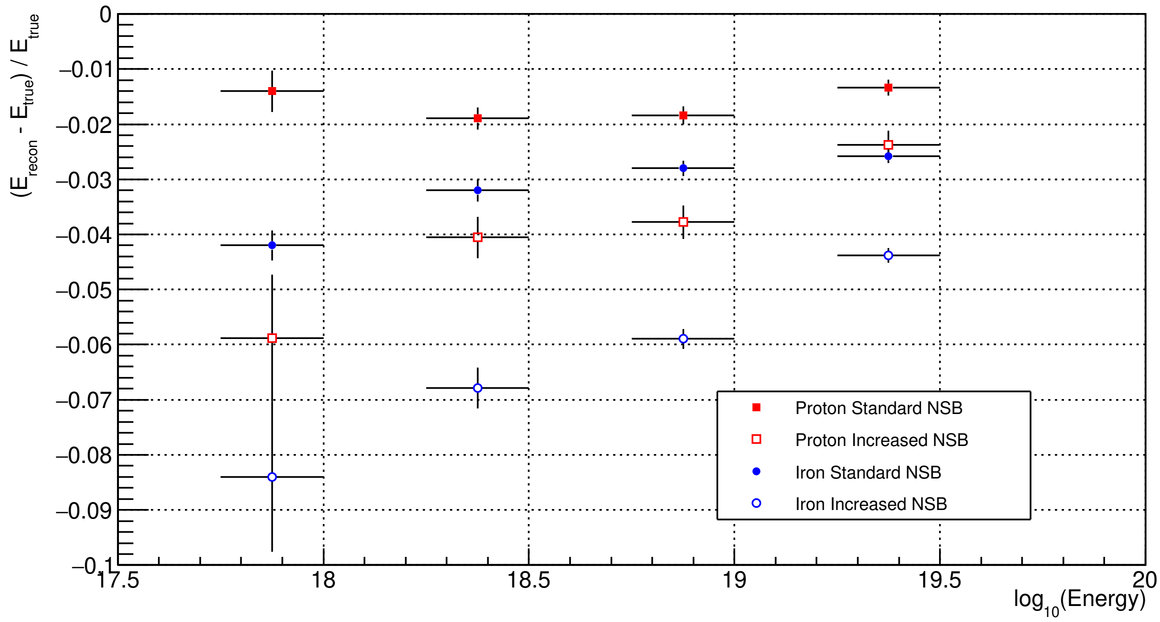

Figure 4.3: Energy Bias using simulated data.

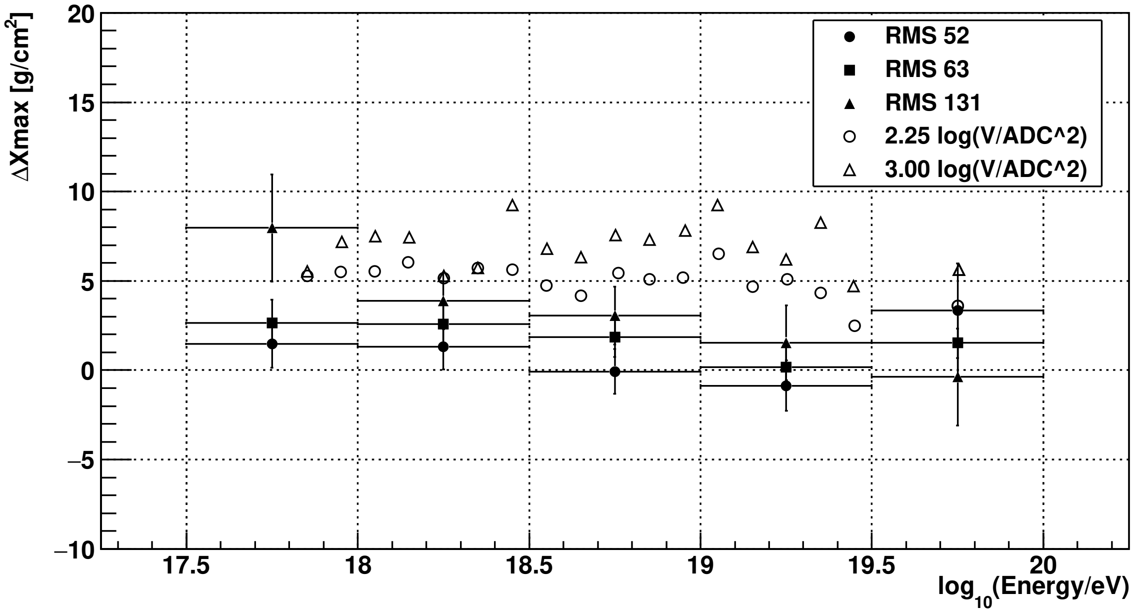

Figure 4.4: Xmax Bias using Smearing Method.

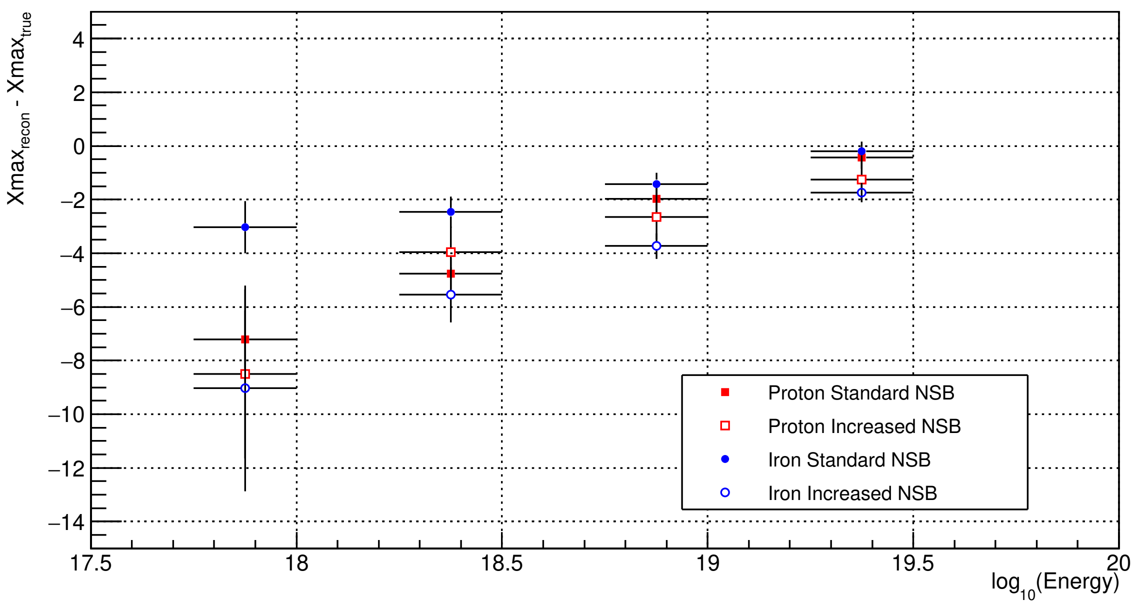

Figure 4.5: Xmax Bias using simulated data.

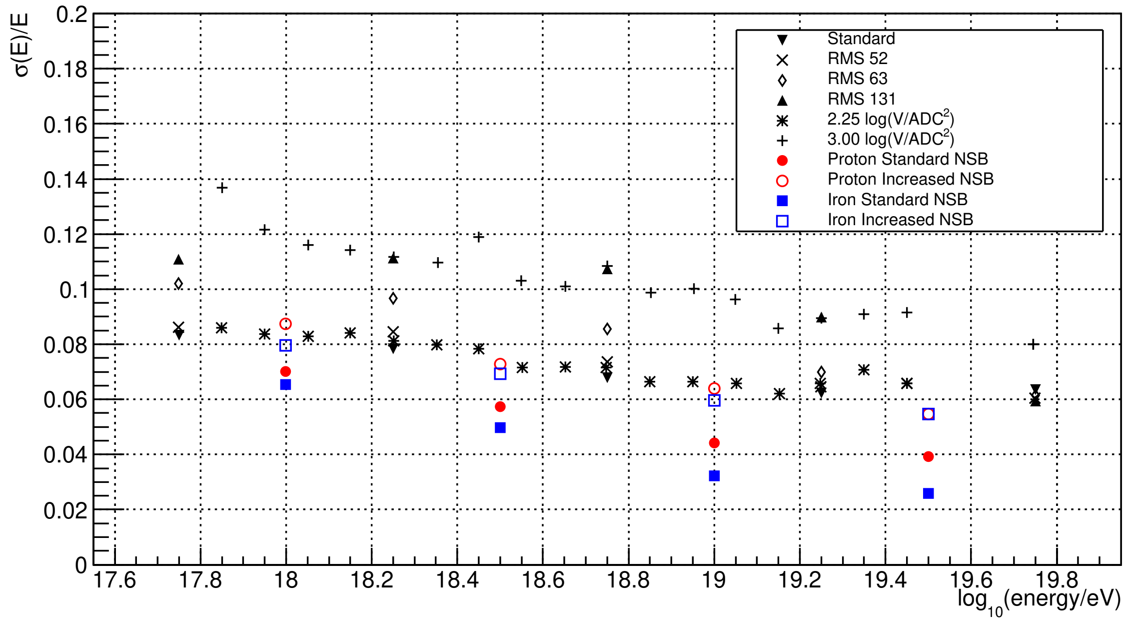

Figure 4.6: Energy Resolution using both Smearing Method data and simulated showers.

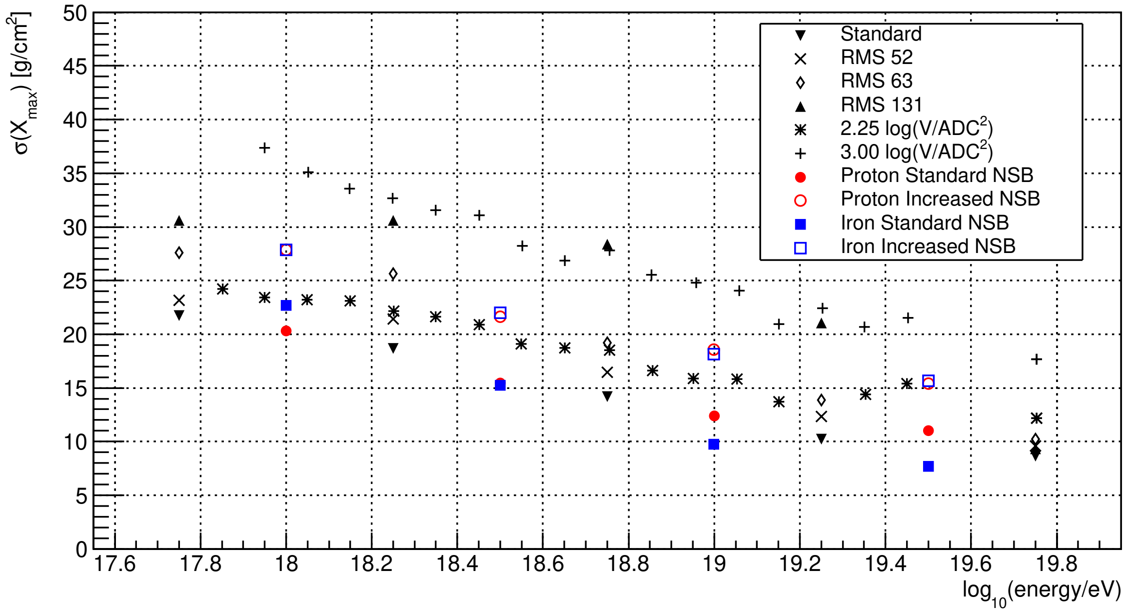

Figure 4.7: Xmax Resolution using both Smearing Method data and simulated showers.

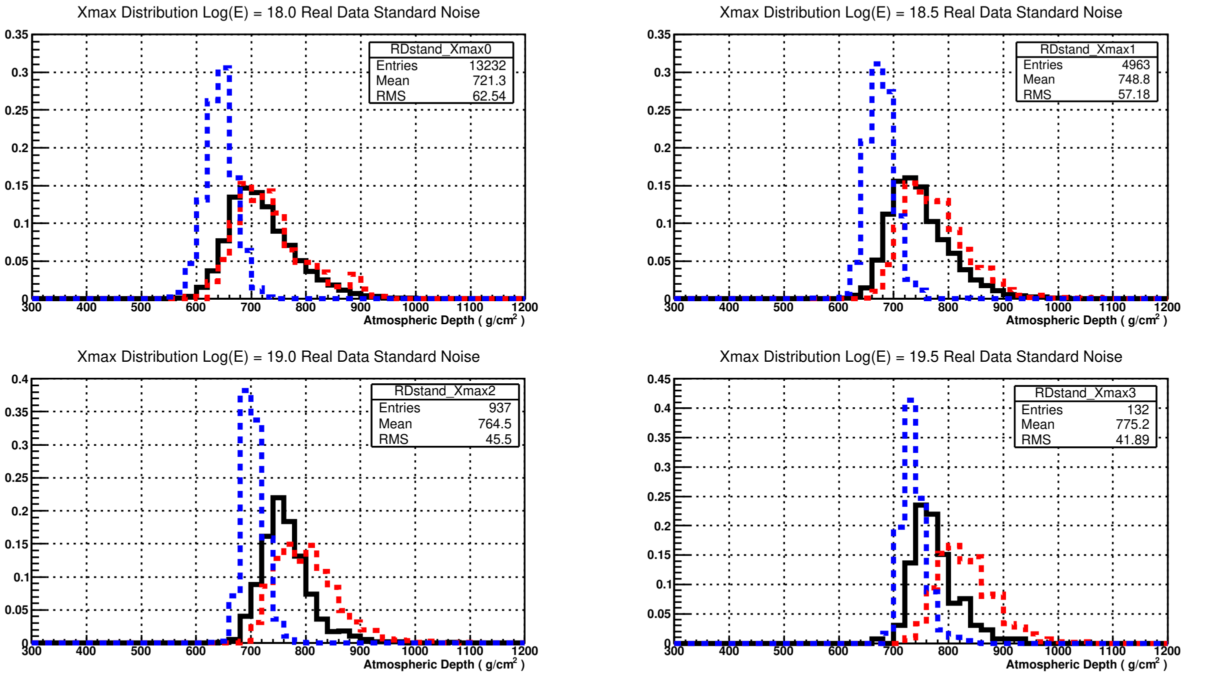

Figure 4.8: Distribution of Xmax with Real Data and simulation of proton and iron showers.

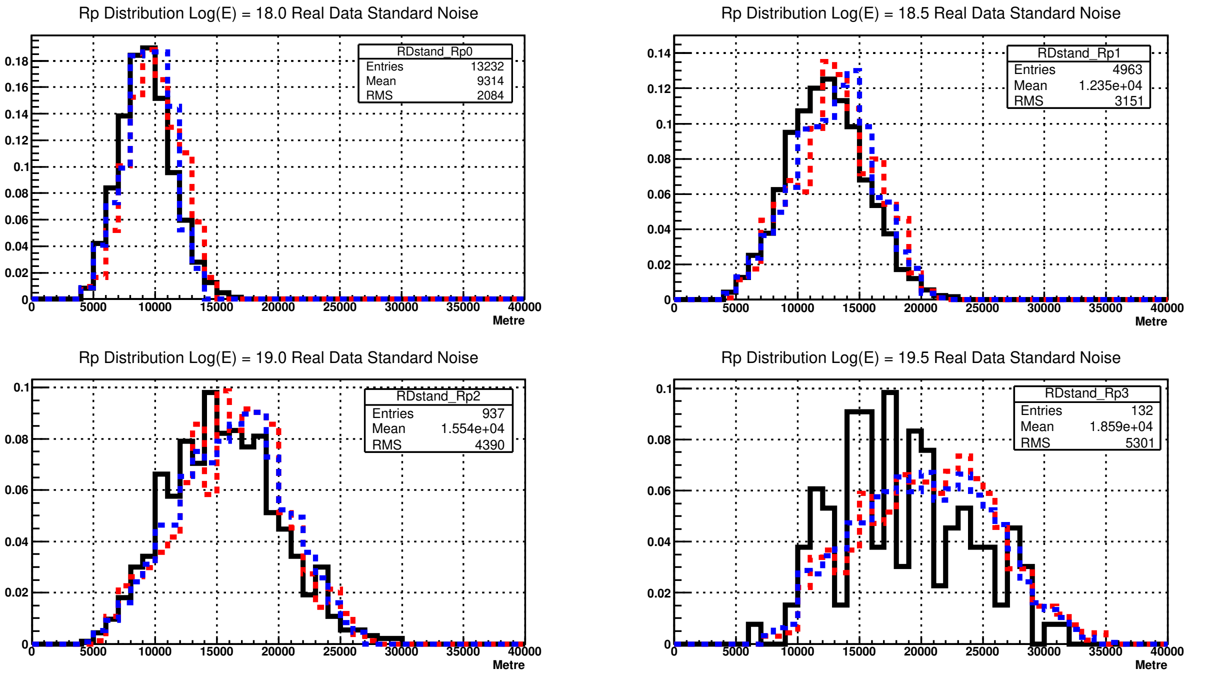

Figure 4.9: Distribution of Rp with Real Data and simulation of proton and iron showers.

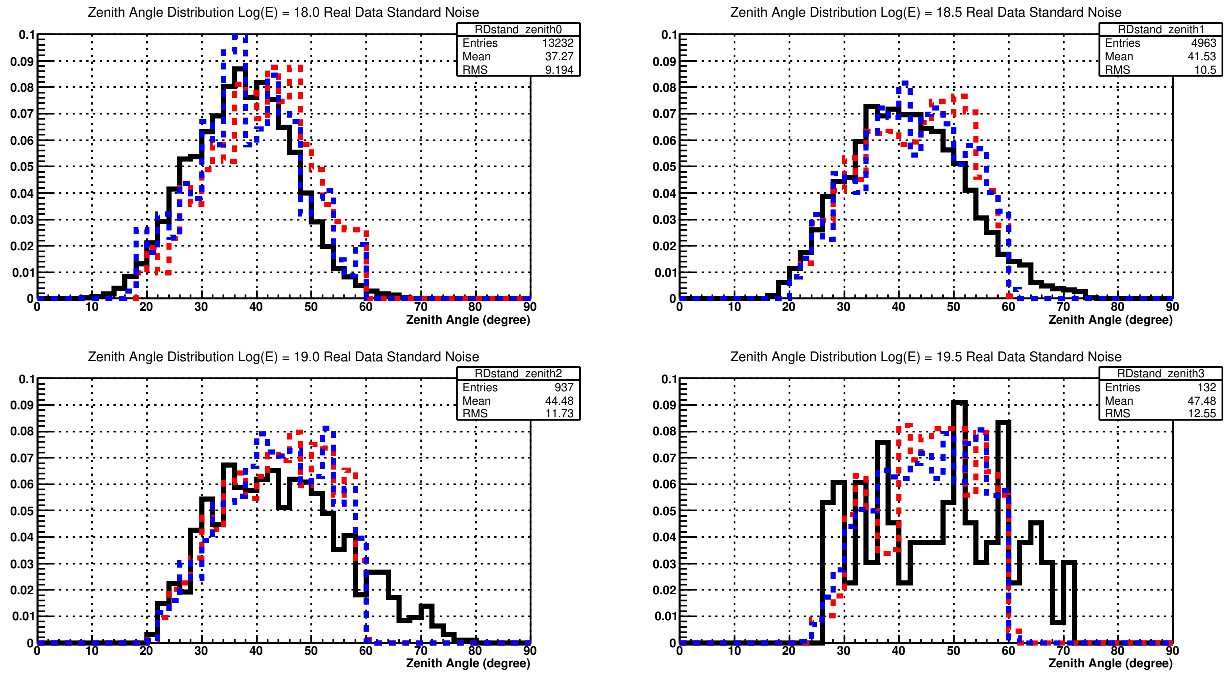

Figure 4.10: Distribution of Zenith angle with Real Data and simulation of proton and iron showers.

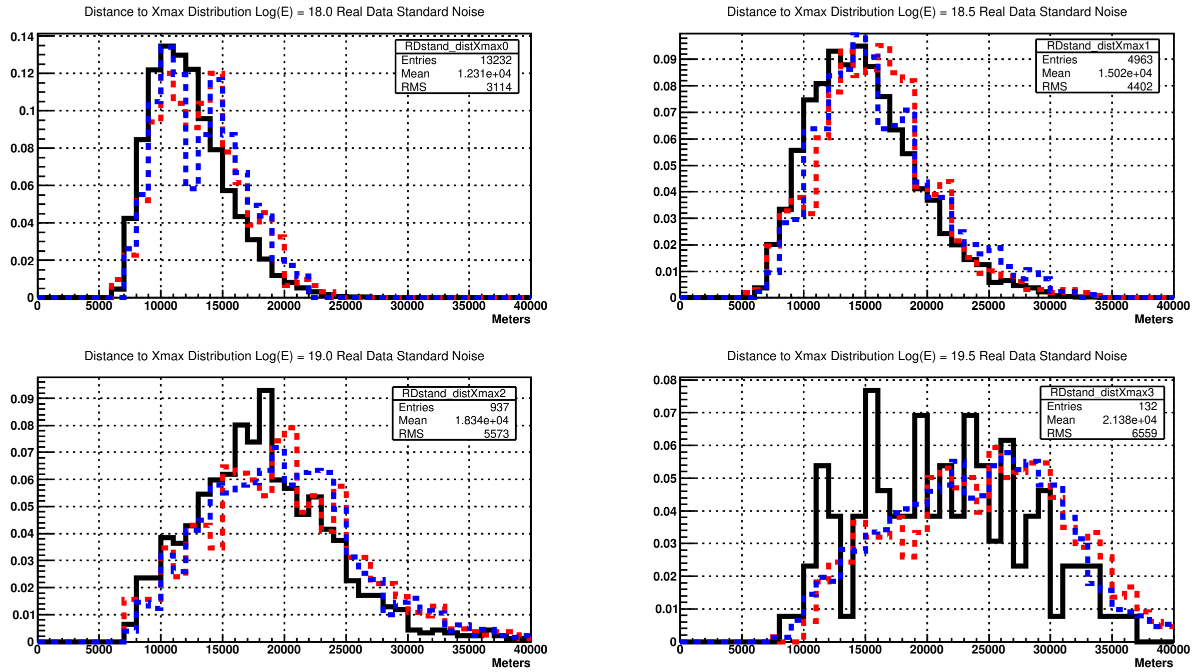

Figure 4.11: Distribution of Distance to Xmax with Real Data and simulation of proton and iron showers.

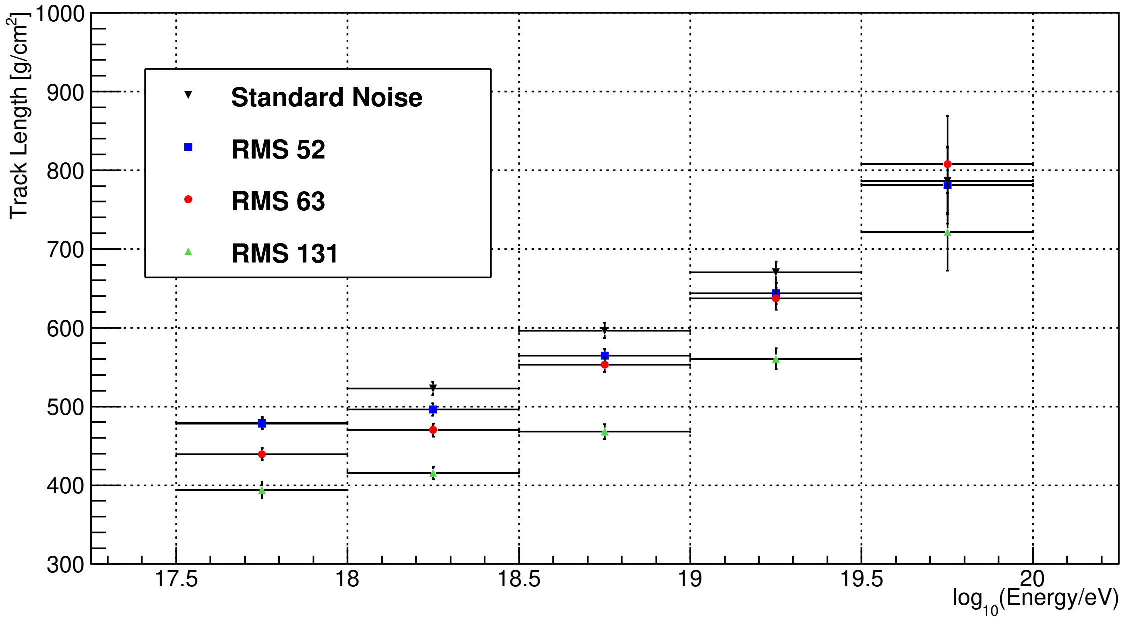

Figure 4.12: Track length using Smearing method.

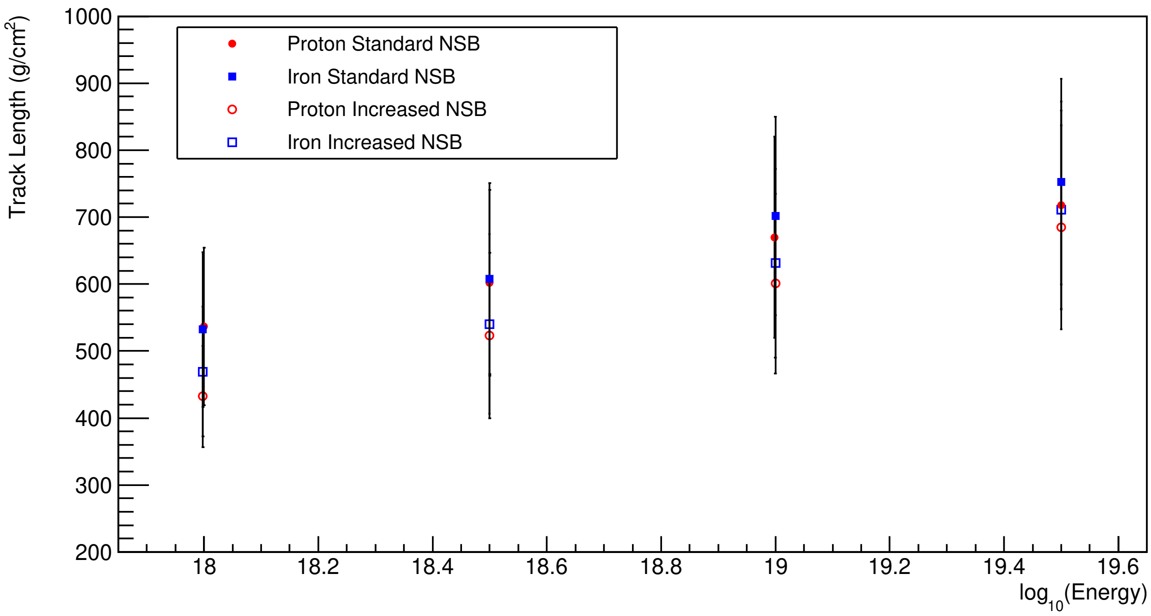

Figure 4.13: Track length using simulation of proton and iron CONEX showers.

Chapter 5

Quantifying Characteristics of the FD PMT

Characterising the PMT at 600V and 900V

- Using the characteristics of the PMT at 900V as a baseline
- Measure linearity
- ND filters vs Two LED method
- Pulse shape?
- temperature effects
- dark noise?

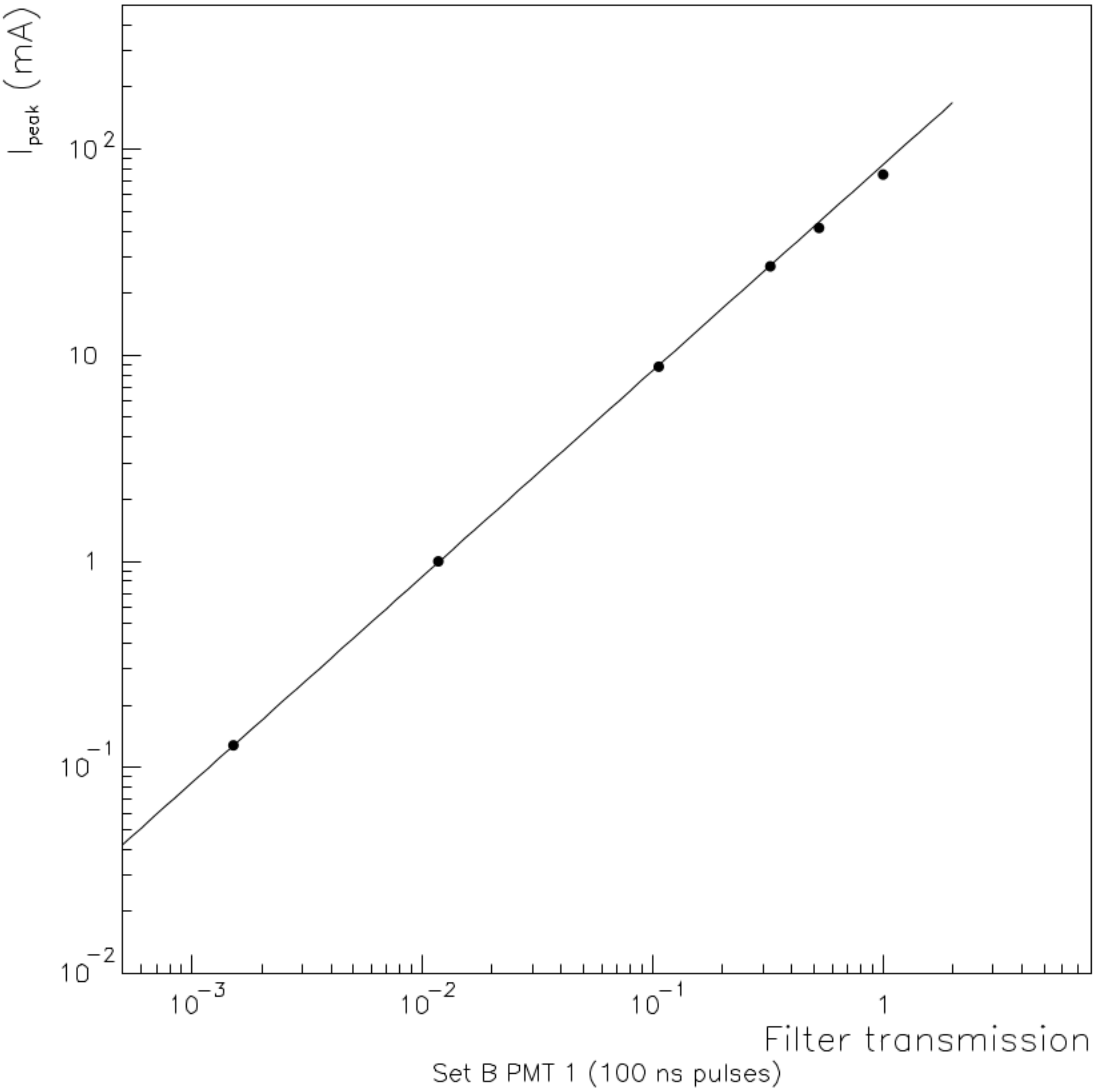

Figure 5.1: Previous PMT linearity test done by Privitera et. al. 1999 with Neutral density filters.

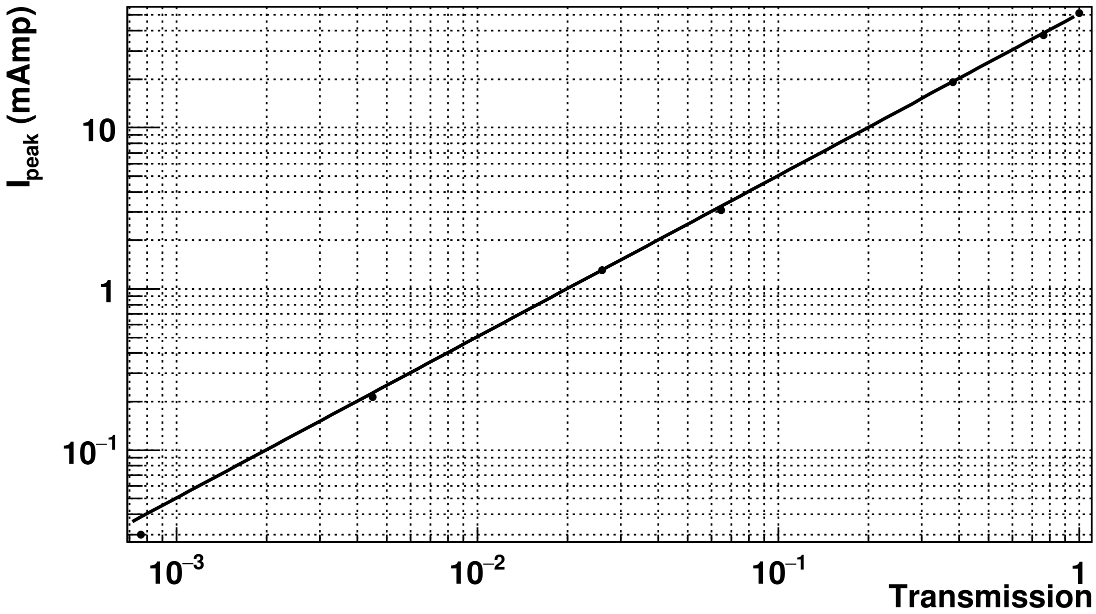

(a)

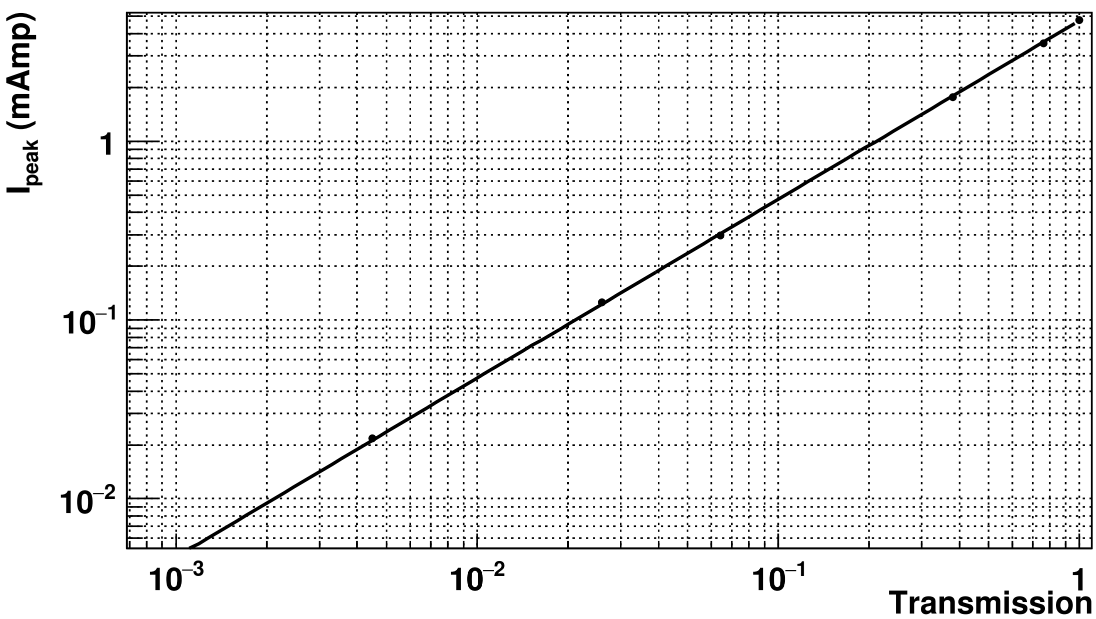

(b)

Figure 5.2: Neutral density method at 900V and 600V.

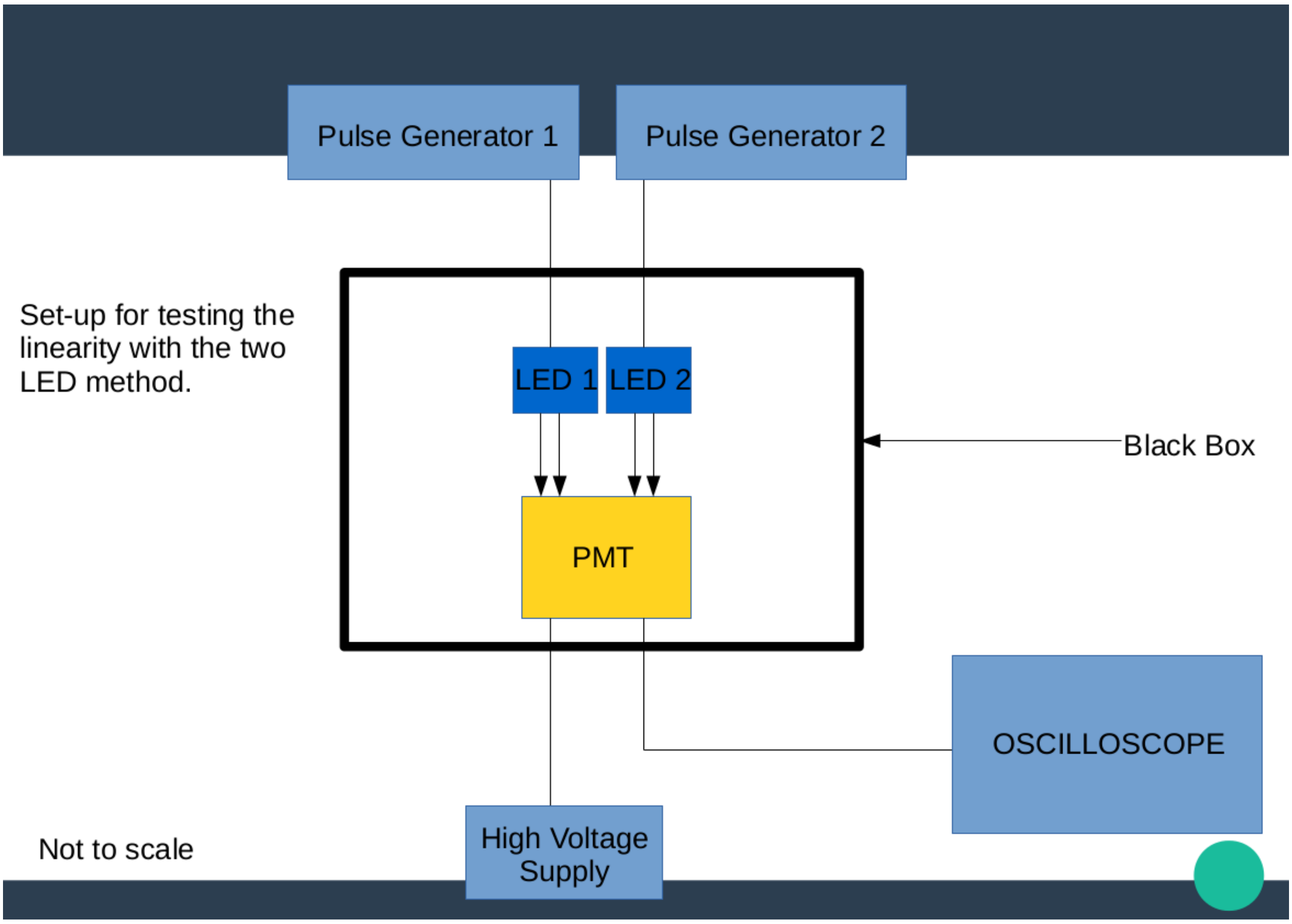
Pulse Generator 1
Pulse Generator 2
Set-up for testing the linearity with the two LED method.
LED 1
LED 2
Black Box
PMT
OSCILLOSCOPE
Not to scale
High Voltage Supply

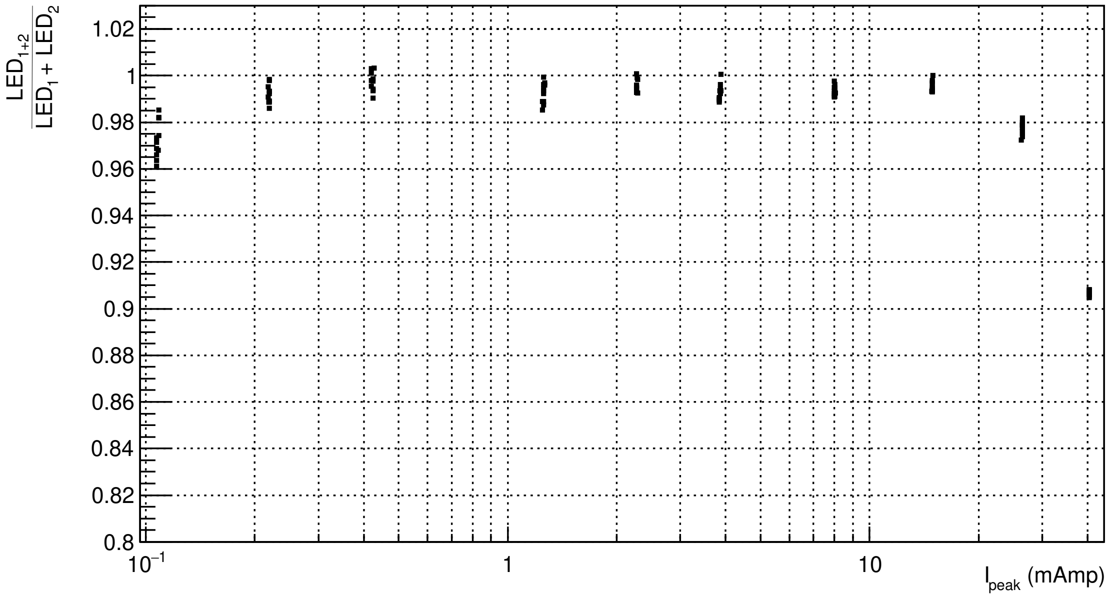

(a)

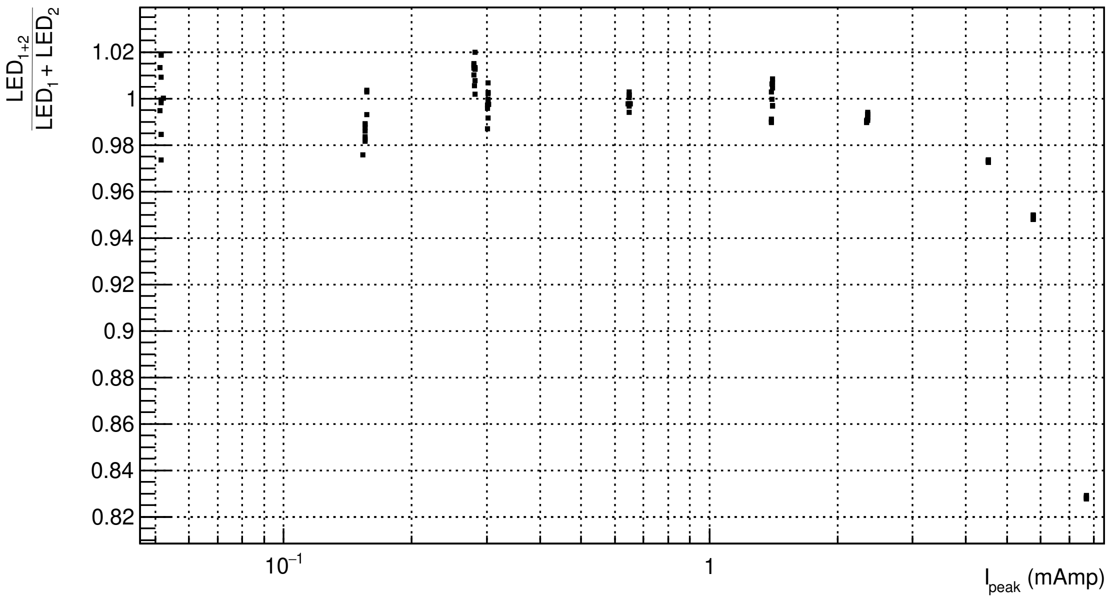

(b)

Figure 5.3: Two LED method at 900V and 600V.

Chapter 6

Computer Simulation of FD PMT

Simulating the FD PMT under differing NSB and for different reasons.

- Theoretical value for Gain Variance
- PMT Gain Variance
- Show both for flat distribution and Gaussian variations for dynodes
- Results
- FD FLT under increased NSB
- Kv simulation under increased NSB?

Chapter 7

Measuring FD PMT Gain Variance with CalA Data

Measuring Gain Variance of FD PMT with CalA Data

- Measuring Gain Variance in the lab did not work. Equipment was not sensitive enough to the low current.
- There was issues with calibrating the LED light source with another PMT (QE curve and wavelength response not the same?)
- Using Low/Standard measurements of CalA to find Gain Variance Ratio
- Three different methods
- Bootstrap method to find uncertainties on Method 3

Chapter 8

Laboratory Simulation of FD shift

Laboratory Simulation of FD shift under differing NSB levels.

- Measurements for both 900V and 600V (900V used as baseline)
- Different length shifts
- Changing NSB
- measuring how the relevant Gain changes throughout a run

Chapter 9

Cloud Camera Cuts Evaluation

First look into the effectiveness of the Cloud Camera cuts on PAO Golen Hybrid data.

- Are we being too conservative?
- Effects on Xmax, Zenith and Rp distributions

Chapter 10

Conclusion

10.1 Future Work

Bibliography

[1] W. Heitler, *The quantum theory of radiation.* Oxford: (Clarendon Press, Ed. 3, Oxford), 1954.